Design of Frequency-Invariant Beamformers Using a Weighted Spatial-Response-Variance Measure

Congwei Feng[1], Huawei Chen[1], Ge Cheng[1,2],Yue Ivan Wu[3]
[1]College of Electronic and Information Engineering, Nanjing University of Aeronautics and Astronautics, China
[2]vivo Mobile Communication Co., Ltd., China
[3]College of Computer Science, Sichuan University, China

***Abstract*—The spatial-response-variance (SRV) is a widely used measure in the design of frequency-invariant (FI) beamformers. Compared with the conventional design approaches for FI-beamformers, there is no need to pre-specify a fixed desired beampattern in the SRV-based design counterparts. Therefore, the SRV-based design approaches enjoy more degrees of freedom (DOFs) than the conventional ones, which contributes to their higher performance in the FI-beamformer design. In this paper, we introduce a weighted SRV measure, which is a generalized version of the SRV, and then propose a weighted-SRV-based FI-beamformer design approach by exploiting the DOFs offered by the weighting coefficients of the weighted SRV. It shows that the FI performance of the resultant beamformers can be further improved compared with the existing SRV-based design. Particularly, array response can be precisely controlled, including mainlobe ripple, sidelobe level and notch depth. Moreover, the weighted-SRV-based design can operate over a wider frequency range, while the SRV-based counterpart may fail.**

***Index Terms*—Frequency invariant beamforming, wideband beamforming, spatial response variance**

I. Introduction

Wideband beamformers have found a wide range of applications in radar, sonar, and audio systems, etc. [1]. It is known that the mainlobe width of conventional wideband beamformers, such as the delay-and-sum beamformers, decreases with frequency. As a result, the signal of interest (SOI) processed by the conventional wideband beamformers will be lowpass filtered when the steering direction of the beamformers deviates from the direction of arrival of the SOI, and hence will lead to distortion of the SOI at the beamformer output. To deal with the problem, many efforts have been made to design the frequency-invariant (FI) beamformers which can achieve a constant mainlobe width [2]–[15].

In the design of FI-beamformers, there usually requires a user-predefined fixed desired beampattern [2]. However, the disadvantage is that it results in the loss of degrees of freedom (DOFs) caused by the arbitrarily-predefined fixed desired beampattern, and thus may sacrifice the FI performance of the synthesized beampatterns. To circumvent the problem, the spatial-response-variance (SRV) measure [16] has drawn much interest in the design of FI-beamformers, which does not need to pre-specify a fixed desired beampattern and hence enjoys more DOFs in the FI-beamformer design. For example, in [17] and [18], a least-squares (LS) approach using the SRV measure for the FI-beamformer design was presented, which is a general approach and can be applied to various array configurations. In [19] and [20], the SRV measure was used in the design of sparse sensor arrays with FI beampatterns.

This research was supported by the National Natural Science Foundation of China under Grant No. 61971219.

In this paper, we first introduce a weighted SRV measure by generalizing the concept of the SRV, and then develop an FI-beamformer design approach based on the weighted SRV. Compared to the existing related works, the main contributions of the paper are summarized as follows:

- A weighted SRV is proposed to design the FI beamformers, and the existing SRV widely used in the current literature can be seen as a special case of the weighted SRV. Accordingly, our proposed design can be regarded as a generalized version of the existing SRV based design.
- By exploiting the weighting functions in the weighted SRV, the proposed design approach offers two advantages. One is that the array response can be precisely controlled, including the mainlobe ripple, sidelobe level and notch depth. In contrast, the existing SRV-based design approaches have no such ability for array response control. And the other advantage is that we can design the FI beamformers with a wider frequency band, while the conventional SRV-based counterpart may fail.
- Regarding the optimization problem based on the weighted SRV, it is rather challenging due to its nonlinear and nonconvex nature. To deal with it, we propose a solution by extending our recent work [22], where only narrowband case is considered. Nevertheless, the extension is not trivial. The algorithm in [22] is not directly applicable to solve the present problem, because the previous algorithm assumes a fixed desired beampattern, while in the present work the desired beampattern is not fixed and instead depends on the beamformer weights.

II. Signal Model

Consider a farfield wideband beamformer with the general filter-and-sum structure for an M-element linear sensor array, where there are L filter taps attached to each sensor. (We would like to point out that, although we consider a linear array, our proposed method is applicable to arbitrary array geometries.) For a plane-wave signal with the normalized angular frequency ω and angle of arrival θ (defined anticlockwise relative to array

axis), the array response of the beamformer, or beampattern, can be expressed as

$$P(\theta,\omega)=\sum_{m=0}^{M-1}\sum_{l=0}^{L-1}w_{m,l}^{\dagger}e^{-j\omega(\tau_m(\theta)f_s+l)} \tag{1}$$

where $w_{m,l}$ denotes the beamformer weight at the lth tap of the mth sensor, $(\cdot)^{\dagger}$ represents complex conjugate, $j=\sqrt{-1}$, f_s is the sampling frequency, and $\tau_m(\theta)$ stands for the propagation time delay between the mth sensor and a reference point.

Using a vector notation, (1) can be rewritten as

$$P(\theta,\omega)=\mathbf{w}^{\mathrm{H}}\mathbf{s}(\theta,\omega) \tag{2}$$

where $[\cdot]^{\mathrm{H}}$ denotes the Hermitian transpose, the beamformer weight vector $\mathbf{w}$ is defined as

$$\mathbf{w}=[w_{0,0},\cdots,w_{M-1,0},\cdots,w_{0,L-1}\cdots,w_{M-1,L-1}]^{\mathrm{T}}, \tag{3}$$

and the steering vector $\mathbf{s}(\theta,\omega)$ is given by

$$\mathbf{s}(\theta,\omega)=\mathbf{s}_1(\omega)\otimes\mathbf{s}_2(\theta,\omega) \tag{4}$$

where $[\cdot]^{\mathrm{T}}$ denotes the transpose, $\otimes$ represents the Kronecker product, $\mathbf{s}_1(\omega)=\left[1,e^{-j\omega},\cdots,e^{-j\omega(L-1)}\right]^{\mathrm{T}}$ and $\mathbf{s}_2(\theta,\omega)=\left[1,e^{-j\omega\tau_1(\theta)f_s},\cdots,e^{-j\omega\tau_{M-1}(\theta)f_s}\right]^{\mathrm{T}}$.

III. Weighted SRV

The SRV is defined as the Euclidean distance between the beampattern at a fixed reference frequency and those at all the other operating frequencies over the angle range of interest [17]. In many scenarios, the FI property is only needed to be considered in the mainlobe region. Mathematically, the SRV measure can be expressed as

$$J_{\mathrm{SRV}}=\sum_{\omega\in\Omega}\sum_{\theta\in\Theta_{\mathrm{ML}}}|\mathbf{w}^{\mathrm{H}}\mathbf{s}(\theta,\omega)-P_{\mathrm{ref}}(\theta,\omega)|^2 \tag{5}$$

where $P_{\mathrm{ref}}(\theta,\omega)=\mathbf{w}^{\mathrm{H}}\mathbf{s}(\theta,\omega_{\mathrm{ref}})$ is the reference beampattern, Ω is the frequency range of interest, Θ_{ML} is the mainlobe region, and ω_{ref} is a reference frequency within Ω.

Based on (5), we propose a weighted SRV measure:

$$J_{\mathrm{WSRV}}=\sum_{\omega\in\Omega}\sum_{\theta\in\Theta_{\mathrm{ML}}}F_{\mathrm{ML}}(\theta,\omega)\left|\mathbf{w}^{\mathrm{H}}\mathbf{s}(\theta,\omega)-P_{\mathrm{ref}}(\theta,\omega)\right|^2 \tag{6}$$

where $F_{\mathrm{ML}}(\theta,\omega)>0$ denotes the weighting coefficients.

The proposed weighted SRV can be seen as a generalized version of the SRV. Specifically, when $F_{\mathrm{ML}}(\theta,\omega)=1$, the weighted SRV degenerates into the SRV.

IV. Proposed FI-Beamformer Design Approach Based on Weighted SRV

A. Problem Formulation

Similar to [17], the FI-beamformer design using the weighted SRV can be cast as a constrained LS problem:

$$\min_{\mathbf{w}}\ J_{\mathrm{WSRV}}+\sum_{\omega\in\Omega}\sum_{\theta\in\Theta_{\mathrm{SL}}}F_{\mathrm{SL}}(\theta,\omega)\left|\mathbf{w}^{\mathrm{H}}\mathbf{s}(\theta,\omega)\right|^2 \tag{7a}$$

$$\text{s.t.}\quad P_{\mathrm{ref}}(\theta_{\mathrm{s}},\omega_{\mathrm{ref}})=1 \tag{7b}$$

where Θ_{SL} denotes the sidelobe region, $F_{\mathrm{SL}}(\theta,\omega)$ is the nonnegative weighting coefficients in Θ_{SL}, and θ_{s} is the look direction. The second term in (7a) is to control the sidelobe level, and the constraint (7b) is to avoid trivial solution.

With (7), our problem can be described as: Refine the solution of (7) by tuning $F_{\mathrm{ML}}(\theta,\omega)$ and $F_{\mathrm{SL}}(\theta,\omega)$ such that

$$\begin{cases}\ ||P(\theta,\omega)|-|P_{\mathrm{ref}}(\theta,\omega)||\le\varepsilon_{\mathrm{ML}}, & (\theta,\omega)\in(\Theta_{\mathrm{ML}},\Omega);\ (8a)\\ \ |P(\theta,\omega)|\le\Gamma_{\mathrm{SL}}(\theta,\omega), & (\theta,\omega)\in(\Theta_{\mathrm{SL}},\Omega)\ (8b)\end{cases}$$

where $\varepsilon_{\mathrm{ML}}$ is the pre-specified mainlobe ripple and $\Gamma_{\mathrm{SL}}(\theta,\omega)$ is the sidelobe level.

B. Solution to the Proposed Design Problem

Note that the optimization problem (7) with the constraints (8) is nonlinear and nonconvex, and the conventional optimization techniques such as convex programming are not suitable to tackle this kind of problem. In the following, we present an iterative algorithm to solve the problem.

1) Initialization: First, we initialize the weighting coefficients as $F_{\mathrm{ML}}(\theta,\omega)\triangleq F_{\mathrm{ML},0}(\theta,\omega)=1$ and $F_{\mathrm{SL}}(\theta,\omega)\triangleq F_{\mathrm{SL},0}(\theta,\omega)=1$. The resultant solution to (7) is denoted as $\mathbf{w}_*$. Accordingly, the reference beampattern can be expressed as $P_{\mathrm{ref}}(\theta,\omega)=\mathbf{w}_*^{\mathrm{H}}\mathbf{s}(\theta,\omega_{\mathrm{ref}})$.

Note that the solution of the SRV-based design, i.e. $\mathbf{w}_*$, generally does not satisfy the design specification (8). Hence, we next develop an iterative procedure to guarantee that (8) holds by further exploiting the DOFs provided by the weighting coefficients. To this end, the initial beamformer weight vector, denoted as $\mathbf{w}_0$, can be obtained by solving the following LS problem:

$$\min_{\mathbf{w}_0}\ \sum_{\omega\in\Omega}\sum_{\theta\in\Theta_{\mathrm{ML}}}|\mathbf{w}_0^{\mathrm{H}}\mathbf{s}(\theta,\omega)-P_{\mathrm{ref}}(\theta,\omega)|^2+\sum_{\omega\in\Omega}\sum_{\theta\in\Theta_{\mathrm{SL}}}|\mathbf{w}_0^{\mathrm{H}}\mathbf{s}(\theta,\omega)|^2. \tag{9}$$

The solution that minimizes (9) is given by

$$\mathbf{w}_0=\mathbf{G}_0^{-1}\boldsymbol{a}_0 \tag{10}$$

where

$$\mathbf{G}_0=\sum_{\omega\in\Omega}\sum_{\theta\in\Theta_{\mathrm{ML}}\cup\Theta_{\mathrm{SL}}}\mathbf{s}(\theta,\omega)\mathbf{s}^{\mathrm{H}}(\theta,\omega) \tag{11}$$

$$\boldsymbol{a}_0=\sum_{\omega\in\Omega}\sum_{\theta\in\Theta_{\mathrm{ML}}}P_{\mathrm{ref}}^{\dagger}(\theta,\omega)\mathbf{s}(\theta,\omega). \tag{12}$$

2) Iteration Steps: At each iteration, we aim to tune the weighting coefficients F_{ML} and F_{SL} at the angle-frequency point where the design specification (8) is most severely violated, i.e., where the beampattern has the largest deviation from the design specification. The iteration steps continue until (8) is finally satisfied.

For the kth ($k\ge1$) iteration, we first search for the angle-frequency point, denoted as (θ',ω'), that violates the design specification (8) most severely, i.e.,

$$(\theta',\omega')=\arg\max_{(\theta,\omega)}\ e_{\max} \tag{13}$$

where

$$e_{\max}=\max\left\{\max_{(\theta,\omega)\in(\Theta_{\rm ML},\Omega)}\big||P_{k-1}(\theta,\omega)|-|P_{{\rm ref},k-1}(\theta,\omega)|\big|\,,\right.$$
$$\left.\max_{(\theta,\omega)\in(\Theta_{\rm SL},\Omega)}|P_{k-1}(\theta,\omega)|-\Gamma_{\rm SL}(\theta,\omega)+\varepsilon_{\rm ML}\right\} \quad (14)$$

with $P_{k-1}(\theta,\omega)=\mathbf{w}_{k-1}^{\rm H}\mathbf{s}(\theta,\omega)$ and $P_{{\rm ref},k-1}(\theta,\omega)=\mathbf{w}_{k-1}^{\rm H}\mathbf{s}(\theta,\omega_{\rm ref})$.

Note that, at the kth iteration, we only focus on the adjustment at one point, i.e., (θ',ω'). However, the reference beampattern at (θ',ω'), i.e., $P_{{\rm ref},k}(\theta',\omega')=\mathbf{w}_k^{\rm H}\mathbf{s}(\theta',\omega_{\rm ref})$, is not available since we have no access to $\mathbf{w}_k$ at the kth iteration. To get around the problem, we use the reference beampattern at the $(k-1)$th iteration instead to approximate the current reference beampattern. Accordingly, the resultant reference beampattern, denoted as $\widetilde{P}_{{\rm ref},k}(\theta,\omega)$, can be expressed as

- If $(\theta',\omega')\neq(\theta_{\rm s},\omega_{\rm ref})$, then

$$\widetilde{P}_{{\rm ref},k}(\theta,\omega)=\begin{cases}P_{{\rm ref},k-1}(\theta,\omega), & (\theta,\omega)=(\theta',\omega'); \quad (15a)\\ \widetilde{P}_{{\rm ref},k-1}(\theta,\omega), & \text{otherwise.} \quad (15b)\end{cases}$$

- Otherwise, we have

$$\widetilde{P}_{{\rm ref},k}(\theta,\omega)=\begin{cases}1, & (\theta,\omega)=(\theta',\omega'); \quad (16a)\\ \widetilde{P}_{{\rm ref},k-1}(\theta,\omega), & \text{otherwise} \quad (16b)\end{cases}$$

where $\widetilde{P}_{{\rm ref},0}(\theta,\omega)=\mathbf{w}_*^{\rm H}\mathbf{s}(\theta,\omega_{\rm ref})$.

With $\widetilde{P}_{{\rm ref},k}(\theta,\omega)$, now the problem becomes to adjust $F_{{\rm ML},k}(\theta',\omega')$ and $F_{{\rm SL},k}(\theta',\omega')$ such that

$$\begin{cases}\big||P_k(\theta',\omega')|-|\widetilde{P}_{{\rm ref},k}(\theta',\omega')|\big|\le\varepsilon_{\rm ML}, (\theta',\omega')\in(\Theta_{\rm ML},\Omega); & (17a)\\ |P_k(\theta',\omega')|\le\Gamma_{\rm SL}(\theta',\omega'), \quad (\theta',\omega')\in(\Theta_{\rm SL},\Omega). & (17b)\end{cases}$$

To guarantee that (17) holds, it can be verified that it suffices to require:

$$\begin{cases}\big||P_k(\theta',\omega')|^2-|\widetilde{P}_{{\rm ref},k}(\theta',\omega')|^2\big|\le\varepsilon'_{\rm ML}, (\theta',\omega')\in(\Theta_{\rm ML},\Omega); & (18a)\\ |P_k(\theta',\omega')|^2\le\Gamma_{\rm SL}^2(\theta',\omega'), \quad (\theta',\omega')\in(\Theta_{\rm SL},\Omega) & (18b)\end{cases}$$

where $\varepsilon'_{\rm ML}=|\varepsilon_{\rm ML}^2-2\varepsilon_{\rm ML}|\widetilde{P}_{{\rm ref},k}(\theta',\omega')||$. To facilitate the analysis, in the following we will consider (18) as an alternative form of (17).

The beamformer weight vector at the kth iteration, $\mathbf{w}_k$, is given by solving the following LS problem:

$$\min_{\mathbf{w}_k}\sum_{\omega\in\Omega}\sum_{\theta\in\Theta_{\rm ML}}F_{{\rm ML},k}(\theta,\omega)|\mathbf{w}_k^{\rm H}\mathbf{s}(\theta,\omega)-\widetilde{P}_{{\rm ref},k}(\theta,\omega)|^2 + \sum_{\omega\in\Omega}\sum_{\theta\in\Theta_{\rm SL}}F_{{\rm SL},k}(\theta,\omega)|\mathbf{w}_k^{\rm H}\mathbf{s}(\theta,\omega)|^2. \quad (19)$$

The solution to (19) can be expressed as

$$\mathbf{w}_k=\mathbf{G}_k^{-1}\boldsymbol{a}_k \quad (20)$$

where

$$\mathbf{G}_k=\sum_{\omega\in\Omega}\sum_{\theta\in\Theta_{\rm ML}}F_{{\rm ML},k}(\theta,\omega)\mathbf{s}(\theta,\omega)\mathbf{s}^{\rm H}(\theta,\omega) + \sum_{\omega\in\Omega}\sum_{\theta\in\Theta_{\rm SL}}F_{{\rm SL},k}(\theta,\omega)\mathbf{s}(\theta,\omega)\mathbf{s}^{\rm H}(\theta,\omega) \quad (21)$$

$$\boldsymbol{a}_k=\sum_{\omega\in\Omega}\sum_{\theta\in\Theta_{\rm ML}}F_{{\rm ML},k}(\theta,\omega)\widetilde{P}_{{\rm ref},k}^{\dagger}(\theta,\omega)\mathbf{s}(\theta,\omega). \quad (22)$$

Suppose that

$$\begin{cases}F_{{\rm ML},k}(\theta',\omega')=F_{{\rm ML},k-1}(\theta',\omega')+\Delta_{F_{\rm ML}} & (23a)\\ F_{{\rm SL},k}(\theta',\omega')=F_{{\rm SL},k-1}(\theta',\omega')+\Delta_{F_{\rm SL}} & (23b)\end{cases}$$

where $\Delta_{F_{\rm ML}}$ and $\Delta_{F_{\rm SL}}$ is the required adjustment in order to ensure that (18) holds. Then, by (21) and (23), we have

$$\mathbf{G}_k=\mathbf{G}_{k-1}+\Delta_F\,\mathbf{s}(\theta',\omega')\mathbf{s}^{\rm H}(\theta',\omega') \quad (24)$$

where

$$\Delta_F=\begin{cases}\Delta_{F_{\rm ML}}, & (\theta',\omega')\in(\Theta_{\rm ML},\Omega);\\ \Delta_{F_{\rm SL}}, & (\theta',\omega')\in(\Theta_{\rm SL},\Omega).\end{cases} \quad (25)$$

Further applying the Woodbury lemma [21] to (24) yields

$$\mathbf{G}_k^{-1}=\mathbf{G}_{k-1}^{-1}-\frac{\Delta_F\mathbf{G}_{k-1}^{-1}\mathbf{s}(\theta',\omega')\,\mathbf{s}^{\rm H}(\theta',\omega')\mathbf{G}_{k-1}^{-1}}{1+\Delta_F\,\mathbf{s}^{\rm H}(\theta',\omega')\mathbf{G}_{k-1}^{-1}\mathbf{s}(\theta',\omega')}. \quad (26)$$

Moreover, by (22) and (23) we can obtain

$$\boldsymbol{a}_k=\begin{cases}\boldsymbol{a}_{k-1}+\Delta_{F_{\rm ML}}\widetilde{P}_{{\rm ref},k}^{\dagger}(\theta',\omega')\mathbf{s}(\theta',\omega')+F_{{\rm ML},k-1}(\theta',\omega') \\ \quad\times\mathbf{s}(\theta',\omega')[\widetilde{P}_{{\rm ref},k}^{\dagger}(\theta',\omega')-\widetilde{P}_{{\rm ref},k-1}^{\dagger}(\theta',\omega')], \\ \qquad\qquad (\theta',\omega')\in(\Theta_{\rm ML},\Omega);\\ \boldsymbol{a}_{k-1}, \qquad\qquad (\theta',\omega')\in(\Theta_{\rm SL},\Omega).\end{cases} \quad (27)$$

With (20), (26) and (27), we can get

$$\mathbf{w}_k=\mathbf{w}_{k-1}+\Delta_{\mathbf{w}} \quad (28)$$

where

$$\Delta_{\mathbf{w}}=\begin{cases}[\widetilde{P}_{{\rm ref},k}^{\dagger}(\theta',\omega')-P_{k-1}^{\dagger}(\theta',\omega')\Delta_{F_{\rm ML}}+F_{{\rm ML},k-1}(\theta',\omega') \\ \times(\widetilde{P}_{{\rm ref},k}^{\dagger}(\theta',\omega')-\widetilde{P}_{{\rm ref},k-1}^{\dagger}(\theta',\omega'))] \\ \times\frac{\mathbf{G}_{k-1}^{-1}\mathbf{s}(\theta',\omega')}{1+\Delta_{F_{\rm ML}}\mathbf{s}^{\rm H}(\theta',\omega')\mathbf{G}_{k-1}^{-1}\mathbf{s}(\theta',\omega')}, \ (\theta',\omega')\in(\Theta_{\rm ML},\Omega);\\ \frac{-\Delta_{F_{\rm SL}}\mathbf{G}_{k-1}^{-1}\mathbf{s}(\theta',\omega')P_{k-1}^{\dagger}(\theta',\omega')}{1+\Delta_{F_{\rm SL}}\mathbf{s}^{\rm H}(\theta',\omega')\mathbf{G}_{k-1}^{-1}\mathbf{s}(\theta',\omega')}, \ (\theta',\omega')\in(\Theta_{\rm SL},\Omega).\end{cases} \quad (29)$$

Next, the problem is reduced to find $\Delta_{F_{\rm ML}}$ and $\Delta_{F_{\rm SL}}$. Apparently, to ensure that (18) holds, it suffices to consider that $\Delta_{F_{\rm ML}}$ and $\Delta_{F_{\rm SL}}$ satisfy:

$$\begin{cases}\big||P_k(\theta',\omega')|^2-|\widetilde{P}_{{\rm ref},k}(\theta',\omega')|^2\big|=\varepsilon'_{\rm ML}, (\theta',\omega')\in(\Theta_{\rm ML},\Omega); & (30a)\\ |P_k(\theta',\omega')|^2=\Gamma_{\rm SL}^2(\theta',\omega'), \quad (\theta',\omega')\in(\Theta_{\rm SL},\Omega). & (30b)\end{cases}$$

Then, solving (30) for $\Delta_{F_{\rm ML}}$ and $\Delta_{F_{\rm SL}}$ yields:

- For $(\theta',\omega')\in(\Theta_{\rm ML},\Omega)$, there exist at least one positive real solution for $\Delta_{F_{\rm ML}}$ satisfying (30a):

$$\begin{cases}\Delta_{F_{{\rm ML},1}}=\dfrac{-\lambda-\sqrt{\lambda^2-(|\widetilde{P}_{{\rm ref},k}(\theta',\omega')|^2-\rho')\gamma^2\sigma}}{(|\widetilde{P}_{{\rm ref},k}(\theta',\omega')|^2-\rho')\gamma^2} & (31a)\\ \Delta_{F_{{\rm ML},2}}=\dfrac{-\lambda+\sqrt{\lambda^2-(|\widetilde{P}_{{\rm ref},k}(\theta',\omega')|^2-\rho')\gamma^2\sigma}}{(|\widetilde{P}_{{\rm ref},k}(\theta',\omega')|^2-\rho')\gamma^2} & (31b)\end{cases}$$

Algorithm 1: Proposed FI-Beamformer Design Approach

Input: $\theta_{\rm s}$, $\omega_{\rm ref}$, $\varepsilon_{\rm ML}$, $\Gamma_{\rm SL}$, and the discretized angle-frequency regions of interest $\Theta_{\rm ML}$, $\Theta_{\rm SL}$ and Ω.
Initialize $F_{\rm ML}(\theta,\omega)=F_{\rm SL}(\theta,\omega)=1$, and calculate the initial reference beampattern $P_{\rm ref}(\theta,\omega)=\mathbf{w}_*^{\rm H}\mathbf{s}(\theta,\omega_{\rm ref})$ by solving (7).
Compute $\mathbf{w}_0$, $\mathbf{G}_0$ and $\mathbf{a}_0$ by (10), (11) and (12).
Set $k=1$ and then compute $e_{\max}$ by (14).
while $e_{\max}>\varepsilon_{\rm ML}$ **do**
  Search for (θ',ω') by (13).
  Compute $\widetilde{P}_{{\rm ref},k}(\theta',\omega')$ by (15) or (16).
  If $(\theta',\omega')\in(\Theta_{\rm ML},\Omega)$, calculate $\Delta_{F_{\rm ML}}$ by (31); otherwise, i.e., $(\theta',\omega')\in(\Theta_{\rm SL},\Omega)$, calculate $\Delta_{F_{\rm SL}}$ by (32).
  Update $\mathbf{w}_k$, $\mathbf{G}_k$ and $\boldsymbol{a}_k$ by (28), (24) and (27).
  Check $e_{\max}$ by (14) , and set $k=k+1$.
end

where

$$\begin{aligned}
\lambda =&({\rm Re}[P_{k-1}(\theta',\omega')\widetilde{P}^{\dagger}_{{\rm ref},k}(\theta',\omega')]-\rho')\gamma+\xi\\
\sigma =&(F_{{\rm ML},k-1}(\theta',\omega')|\eta|\gamma)^2+|P_{k-1}(\theta',\omega')|^2-\rho'\\
&+2F_{{\rm ML},k-1}(\theta',\omega'){\rm Re}[P_{k-1}(\theta',\omega')\eta\gamma]\\
\gamma =&\mathbf{s}^{\rm H}(\theta',\omega')\mathbf{G}_{k-1}^{-1}\mathbf{s}(\theta',\omega')\\
\rho' =&\begin{cases}|\widetilde{P}_{{\rm ref},k}(\theta',\omega')|^2+\varepsilon'_{\rm ML}, & \beta>0 \text{ or } (\beta=0,\\ & \quad |P_{k-1}(\theta',\omega')|>|\widetilde{P}_{{\rm ref},k}(\theta',\omega')|)\\ |\widetilde{P}_{{\rm ref},k}(\theta',\omega')|^2-\varepsilon'_{\rm ML}, & \beta<0 \text{ or } (\beta=0,\\ & \quad |P_{k-1}(\theta',\omega')|<|\widetilde{P}_{{\rm ref},k}(\theta',\omega')|)\end{cases}\\
\xi =&\gamma^2F_{{\rm ML},k-1}(\theta',\omega'){\rm Re}[\widetilde{P}_{{\rm ref},k}(\theta',\omega')\eta]\\
\eta =&\widetilde{P}^{\dagger}_{{\rm ref},k}(\theta',\omega')-\widetilde{P}^{\dagger}_{{\rm ref},k-1}(\theta',\omega')\\
\beta =&({\rm Re}[P_{k-1}(\theta',\omega')\widetilde{P}^{\dagger}_{{\rm ref},k}(\theta',\omega')]-|\widetilde{P}_{{\rm ref},k}(\theta',\omega')|^2)\\
&\times\gamma+\xi
\end{aligned}$$

with ${\rm Re}[\cdot]$ representing the real part. Note that, in the case of two feasible solutions $\Delta_{F_{{\rm ML},1}}$ and $\Delta_{F_{{\rm ML},2}}$, we will choose the one with the smaller cost function value (19) as the preferable solution.

- For $(\theta',\omega')\in(\Theta_{\rm SL},\Omega)$, it follows that when

$$\Delta_{F_{\rm SL}}=\frac{|P_{k-1}(\theta',\omega')|/\Gamma_{\rm SL}(\theta',\omega')-1}{\mathbf{s}^{\rm H}(\theta',\omega')\mathbf{G}_{k-1}^{-1}\mathbf{s}(\theta',\omega')},\qquad(32)$$

(30b) holds.

The derivations of (31) and (32) can be obtained by extending our recent work in [22], and thus omitted here.

To summarize, the steps of the proposed FI-Beamformer design approach are shown in Algorithm 1.

V. Design Examples

This section shows some simulation results to compare the proposed design with the existing SRV-based counterpart [17] (i.e., via solving Eq. (21) in [17]). Note that the proposed design can explicitly control the sidelobe level. In the SRV-based design, the sidelobe level is implicitly controlled via a regularization term in the cost function. To facilitate the comparison, we have reformulated the SRV-based design using an explicit sidelobe level constraint, i.e.,

$$\begin{aligned}
\min_{\mathbf{w}}\quad&\sum_{\theta\in\Theta_{\rm ML}}\sum_{\omega\in\Omega}|\mathbf{w}^{\rm H}\mathbf{s}(\theta,\omega)-\mathbf{w}^{\rm H}\mathbf{s}(\theta,\omega_{\rm ref})|^2 &(33a)\\
\text{s.t.}\quad&\mathbf{w}^{\rm H}\mathbf{s}(\theta_{\rm s},\omega_{\rm ref})=1 &(33b)\\
&|\mathbf{w}^{\rm H}\mathbf{s}(\theta,\omega)|\le\Gamma_{\rm SL}(\theta,\omega),\quad(\theta,\omega)\in(\Theta_{\rm SL},\Omega). &(33c)
\end{aligned}$$

Following [17], we consider a 10-sensor uniform linear array with each sensor followed by a 20-tap FIR filter. The inter-sensor spacing is half the wavelength corresponding to the maximum normalized frequency π.

A. Example 1

In the first example, the design specifications are: 1) The mainlobe region $\Theta_{\rm ML}=[60^\circ,120^\circ]$ and the sidelobe region $\Theta_{\rm SL}=[0^\circ,50^\circ]\cup[130^\circ,180^\circ]$; 2) The look direction $\theta_{\rm s}=90^\circ$, and the frequency range $\Omega=[0.25\pi,0.75\pi]$ with the reference frequency $\omega_{\rm ref}=0.7\pi$; 3) The mainlobe ripple $\varepsilon_{\rm ML}=0.3$ dB, and the sidelobe level $\Gamma_{\rm SL}=-30$ dB.

The synthesized beampatterns of the weighted-SRV- and SRV-based designs are shown in Figs. 1(a) and 1(b), respectively, where the mainlobe ripples are shown in the insets. As can be seen, although the SRV-based design can achieve good FI performance, its mainlobe ripple (0.4758 dB) slightly violates the design specification, i.e., 0.3 dB. In comparison, the proposed design can achieve better FI performance, with its mainlobe ripple (0.2369 dB) within the pre-specified threshold. Moreover, the proposed design can also achieve a lower sidelobe level of -37.8615 dB.

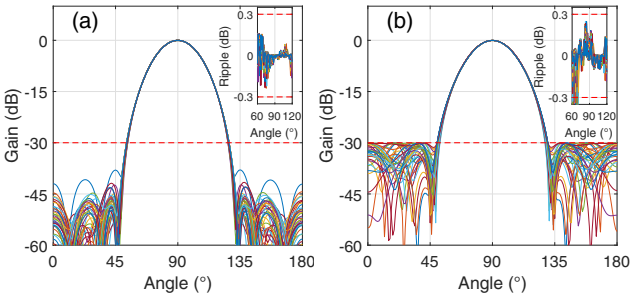

Fig. 1. Synthesized beampatterns of Example 1 with the frequency range $[0.25\pi,0.75\pi]$: (a) weighted-SRV and (b) SRV, where the mainlobe ripples are shown in the insets.

B. Example 2

In the second example, we demonstrate the capability of the weighted-SRV-based approach in the design of FI-beamformers with non-uniform sidelobe levels. The design specifications are same as those in Example 1, except that there is a notch region $[15^\circ,35^\circ]$ with a depth of -45 dB.

Figs. 2(a) and 2(b) plot the synthesized beampatterns of the weighted-SRV- and SRV-based designs, respectively. We can see from Fig. 2 that, with the non-uniform sidelobe

level constraint, the weighted-SRV-based design also performs better than its SRV-based counterpart in terms of the FI performance. The mainlobe ripple of the weighted SRV-based design is 0.2876 dB, which is well below the pre-specified threshold, 0.3 dB. In comparison, the mainlobe ripple of the SRV-based design is 2.6623 dB, which greatly violates the design specification.

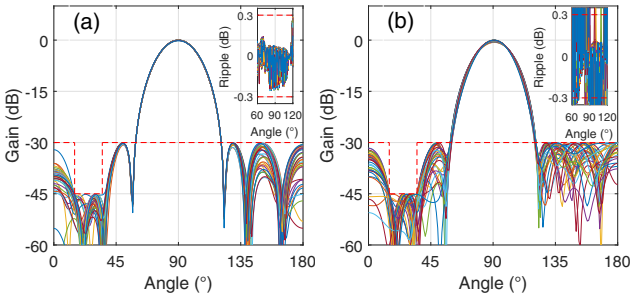

Fig. 2. Synthesized beampatterns of Example 2 with a frequency range $[0.25\pi, 0.75\pi]$ and a notch in the region $[15°, 35°]$: (a) weighted-SRV, (b) SRV, where the mainlobe ripples are shown in the insets.

C. Example 3

In the third example, we increase the frequency band to $\Omega = [0.125\pi, \pi]$. And the remaining design specifications are same as in Example l. Figs. 3(a) and 3(b) show, respectively, the synthesized beampatterns of the weighted-SRV- and SRV-based designs. We can see clearly that the SRV-based design fails to work with a wider frequency range, with its mainlobe ripple up to 17.4831 dB. In contrast, our proposed design performs well with all the design specifications being satisfied, and the mainlobe ripple is just 0.2989 dB.

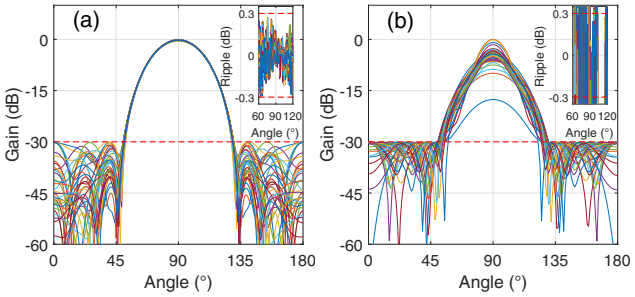

Fig. 3. Synthesized beampatterns of Example 3 with the frequency range $[0.125\pi, \pi]$: (a) weighted-SRV and (b) SRV, where the mainlobe ripples are shown in the insets.

VI. Conclusion

In this paper, we have proposed a weighted-SRV-based approach for the design of FI beamformers. Compared with the existing SRV-based design, the advantage of the proposed approach lies in that it has fully utilized the DOFs offered by the weighting coefficients of the weighted SRV measure. It has shown that the weighted-SRV-based design can achieve better FI performance than the SRV-based design. Particularly, array response can be precisely controlled by the proposed design. Moreover, the proposed design is able to be applicable for a wider frequency range, while the SRV-based design may fail.

References

[1] W. Liu and S. Weiss, Wideband Beamforming: Concepts and Techniques, Chichester, U.K.: Wiley, 2010.

[2] D. Ward, R. Kennedy, and R. Williamson, "Theory and design of broadband sensor arrays with frequency invariant far-field beam patterns," J. Acoust. Soc. Amer., vol. 97, no. 2, pp. 1023–1034, 1995.

[3] T. Chou, "Frequency-independent beamformer with low response error," in Proc. Int. Conf. Acoustics, Speech, Signal Process. IEEE, 1995, vol. 5, pp. 2995–2998.

[4] S. Yan, "Optimal design of FIR beamformer with frequency invariant patterns," Appl. Acoust., vol. 67, no. 6, pp. 511–528, 2006.

[5] W. Liu and S. Weiss, "Design of frequency invarint beamformers for broadband arrays," IEEE Trans. Signal Process., vol. 56, no. 2, pp. 855–860, 2008.

[6] M. Crocco and A. Trucco, "Design of robust superdirective arrays with tunable tradeoff between directivity and frequency-invariance," IEEE Trans. Signal Process., vol. 59, no. 5, pp. 2169–2181, 2011.

[7] Y. Liu, L. Chen, C. Zhu, Y. L. Ban, and Y. J. Guo, "Efficient and accurate frequency-invariant beam pattern synthesis utilizing iterative spatiotemporal fourier transform," IEEE Trans. Antennas Propagat., vol. 68, no. 8, pp. 6069–6079, 2020.

[8] S. C. Chan and H. H. Chen, "Uniform concentric circular arrays with frequency-invariant characteristics-theory, design, adaptive beamforming and doa estimation," IEEE Trans. Signal Process., vol. 55, no. 1, pp. 165–177, 2007.

[9] W. Liu, D. C. McLernon, and M. Ghogho, "Design of frequency invariant beamformer without temporal filtering," IEEE Trans. Signal Process., vol. 57, no. 2, pp. 798–802, 2009.

[10] Y. Gong, S. Xiao, and B. Wang, "Synthesis of nonuniformly spaced arrays with frequency-invariant shaped patterns by sequential convex optimization," IEEE Antennas Wireless Propag. Lett., vol. 19, no. 7, pp. 1093–1097, 2020.

[11] Y. Liu, L. Zhang, C. Zhu, and Q. H. Liu, "Synthesis of nonuniformly spaced linear arrays with frequency-invariant patterns by the generalized matrix pencil methods," IEEE Trans. Antennas Propagat., vol. 63, no. 4, pp. 1614–1625, 2015.

[12] J. Chen, G. Huang and J. Benesty, "On the design of robust steerable frequency-invariant beampatterns with concentric circular microphone arrays," in Proc. Int. Conf.Acoustics, Speech, Signal Process. IEEE, 2018, pp. 506–510.

[13] S. Yan, Y. Ma, and C. Hou, "Optimal array pattern synthesis for broadband arrays," J. Acoust. Soc. Amer., vol. 122, no. 5, pp. 2686–2696, 2007.

[14] B. H. Wang, Y. Guo, Y. L. Wang, and Y. Z. Lin, "Frequency-invariant pattern synthesis of conformal array antenna with low cross-polarisation," IET Microw., Antennas Propag., vol. 2, no. 5, pp. 442–450, 2008.

[15] L. Chen, Y. Liu, S. Yang, and Y. J. Guo, "Efficient synthesis of filter-and-sum array with scanned wideband frequency-invariant beam pattern and space-frequency notching," IEEE Signal Process. Lett., vol. 28, pp. 384–388, 2021.

[16] H. Duan, B. P. Ng, C. M. See, and J. Fang, "Applications of the SRV constraint in broadband pattern synthesis," Signal Process., vol. 88, no. 4, pp. 1035–1045, 2008.

[17] Y. Zhao, W. Liu, and R. Langley, "Application of the least squares approach to fixed beamformer design with frequency-invariant constraints," IET signal process., vol. 5, no. 3, pp. 281–291, 2011.

[18] W. Liu Y. Zhao and R. Langley, "A least squares approach to the design of frequency-invariant beamformers," in Proc. 17th Eur. Signal Process. Conf. (EUSIPCO), 2009, pp. 844–848.

[19] Y. Liu, L. Zhang, L. Ye, Z. Nie, and Q. H. Liu, "Synthesis of sparse arrays with frequency-invariant-focused beam patterns under accurate sidelobe control by iterative second-order cone programming," IEEE Trans. Antennas Propagat., vol. 63, no. 12, pp. 5826–5832, 2015.

[20] M. B. Hawes and W. Liu, "Sparse array design for wideband beamforming with reduced complexity in tapped delay-lines," IEEE/ACM Trans. Audio, Speech, Lang. Process., vol. 22, no. 8, pp. 1236–1247, 2014.

[21] G. H. Golub and C. F. V. Loan, Matrix Computations, Baltimore, The Johns Hopkins Univ. Press, 1996.

[22] G. Cheng and H. Chen, "An analytical solution for weighted least-squares beampattern synthesis using adaptive array theory," IEEE Trans. Antennas Propagat., vol. 69, no. 9, pp. 6034–6039, 2021.